Clean Techn Environ Policy (2013) 15:967–975
DOI 10.1007/s10098-012-0558-2

ORIGINAL PAPER

Co_3O_4 doped over SBA 15: excellent adsorbent materials for the removal of methyleneblue dye Pollutant

P. V. Suraja · Z. Yaakob · N. N. Binitha · S. Triwahyono · P. P. Silija

Received: 11 April 2012 / Accepted: 21 November 2012 / Published online: 1 December 2012

Abstract Nanosized cobalt oxide particles are incorporated into SBA 15 mesoporous silica materials and are effectively used for the first time as adsorbent materials for aquatic dye pollutant removal. Cobalt is found to exist in its Co_3O_4 spinel structure as evident from FTIR and X-ray diffraction studies. The best weight ratio of metal loading to show excellent adsorption of methyleneblue is found to be 10 wt% Co over the support. There, Co_3O_4 spinel nanoparticles lie inside the pores of mesoporous silica. Further increase in the percentage of metal loading decreases the adsorption capacity which may be due to the agglomeration of nanoparticles over the silica support as evident from TEM photographs. Cobalt-doped systems of the present study, having good adsorption capacity of methyleneblue, are prepared via impregnation of cobalt nitrate over SBA 15 in aqueous medium. Here, we introduce a new SBA 15-based system for the fast removal of aquatic dye pollutants which is highly economical for industrial applications.

Keywords Cobalt oxide spinel · SBA 15 · Adsorption · Aquatic pollution · Waste water treatment · Dye removal

P. V. Suraja · Z. Yaakob · P. P. Silija
Department of Chemical and Process Engineering, Faculty of Engineering and Built Environment, Universiti Kebangsaan Malaysia, 43600 UKM Bangi, Selangor, Malaysia

N. N. Binitha (✉)
Department of Chemistry, Sree Neelakanta Government Sanskrit College Pattambi, Palakkad 679306, Kerala, India
e-mail: binithann@yahoo.co.in

S. Triwahyono
Ibnu Sina Institute for Fundamental Science Studies, Faculty of Science, Universiti Teknologi Malaysia, 81310 UTM Johor Bahru, Johor, Malaysia

Introduction

Development of sustainable environment needs two major requirements: limited formation of waste as well as treatment of waste materials once it is formed. Dyes are an important class of aquatic pollutants which cause danger to the environment. Two important methods adopted for dye removal include (1) biochemical oxidation which suffers from significant limitation since most dyestuffs commercially available have been intentionally designed to resist aerobic microbial degradation and are converted to toxic or carcinogenic compounds, and (2) photodegradation over TiO_2 (also some other transition metal oxides) that requires UV light which is highly economical and harmful. Now, there are methods such as anion doping/metal loading to shift the absorption wavelength of TiO_2 to the visible region among which anion doping such as doping with nitrogen succeed in this matter. But, the stability of these catalysts is questionable since the dopant exists as NO, NH_3, N_2, etc. (Peng et al. 2008; Asahi et al. 2001; Popa et al. 2010), and the photocatalyst may get deactivated when we keep the it for long time. Industry gives limited importance for waste treatment since it is always costly and time consuming. Even if we use anion-doped TiO_2, the process to remove pollutants such as dyes requires continuous irradiation using visible light for long duration of time (Apetrei et al. 2009; He et al. 2010; Wang et al. 2010) and still, in most of the cases, the pollutant removal is not reaching to 100 %.

Adsorption is one of earliest solutions for the waste removal. Removal of cationic dyes, such as methyleneblue, from wastewater can be achieved by adsorption onto solid surfaces. The process is simple and only requires mixing of the adsorbent with dye solution which can then be removed by filtration. The widely studied solid adsorbent is activated

carbon. However, the microporous structure of the activated carbon results in slow adsorption kinetics and low adsorption capacity of bulky molecules. In order to overcome the above limitations, many other solid materials such as mesoporous silicas were also investigated as adsorbents (Wang and Li 2006; Anbia and Hariri 2010; Moriguchi et al. 2004; Ren et al. 2007). The selection of mesoporous silicas as adsorbents and supports for metal oxides lies in their very high specific surface area and uniform pore dimension allowing the patterning of small and well-calibrated oxide particles/adsorbates. Among the different mesoporous silicas, SBA 15, the structured silica materials similar to MCM-41, exhibits larger pore size, thicker pore wall, higher thermal, and hydrothermal stabilities. Mesoporous SBA 15 is also found to be a good adsorbent for MB (Huang et al. 2011). Joo et al. (2009) used PDDA-modified SBA-15 for the selective adsorption of anionic dyes from the aqueous solution and found that PDDA-modified SBA-15 has a larger adsorption capacity than PDDA-modified commercial silica and granular activated carbon.

In the present work, we aim to check the complete removal of dye pollutants by adsorption over cobalt metal oxide incorporated SBA 15, for the first time. Cobalt nitrate aqueous solution is used as the precursor for the metal incorporation. Efficient dispersion of Co_3O_4 spinel over SBA 15 is achieved by impregnation method. Influence of the percentage metal loading on the properties as well as in adsorption capacity of a model aquatic pollutant, methyleneblue is investigated. It is found that the present adsorbent materials are highly efficient that can remove the dyes simply by mixing for about 10 min time and thus can be effectively used for industrial applications.

Materials and methods

Preparation of SBA-15

The support SBA-15 material is prepared by the method already reported (Lee et al. 2009). Two gram of triblock polymer-P123 ($M_w = 5800$, Aldrich) was dissolved in a mixture of distilled water (15 mL) and 2 M HCl (60 mL) (R&M chemicals). To that solution, 4.25 g TEOS (Aldrich) was added and then stirred at 45 °C for 20 h. The mixture was aged at 85 °C for overnight. The filtered material was dried under vacuum at room temperature for overnight and then calcined at 550 °C for 6 h.

Preparation of cobalt-loaded SBA 15

Cobalt loading was done on SBA 15 by simple impregnation method. The cobalt nitrate hexahydrate (Hamburg Chemical GmbH) was first dissolved in water to get a 0.0286 M solution. A predetermined amount of prepared SBA 15 was then added to this solution, followed by heating at 85 °C for removal of the solvent. The amount of cobalt nitrate solution was varied to get different wt% of cobalt (5–50 %)/g SBA in each impregnation. The concentrated sample was dried in oven at 85 °C for overnight. The dried samples were calcined at 500 °C for 3 h. The adsorbents are designated as 5CoSBA, 10CoSBA, 20CoSBA, 30CoSBA, 40CoSBA, and 50CoSBA where the numbers indicates the weight percentage metal loading. In order to permit a perfect comparison of efficiency, a solution of cobalt nitrate was evaporated under stirring at 85 °C which is then calcined at 400 °C to generate cobalt oxides to make the physical blends of 10 wt% cobalt oxides and SBA-15. The blend is then calcined at 500 °C for 3 h.

Adsorbent characterization

XRD patterns of the samples were recorded for 2θ between 3° and 80° on a Bruker AXS D8 Advance diffractometer employing a scanning rate of 0.02°/s with Cu K_α radiation ($\lambda = 1.5418$). The FTIR spectra were recorded in NICOLET6700 FT-IR Thermoscientific in the region 400–4,000 cm^{-1}. Diffuse Reflectance Ultraviolet–Visible spectral (UV–Vis DRS) studies of powder adsorbent samples was carried out at room temperature using a Varian, Cary spectrophotometer in the range of 200–800 nm. The dispersion of cobalt oxide on support was studied from TEM images (Jeol JEM2100 electron microscope). SEM morphology of prepared adsorbent was taken in a Jeol 6390LV scanning electron microscope. BET surface area and pore volume were measured using TriStar 3000 V6.04 A by nitrogen physisorption at −195.800 °C. The pore size distribution and pore volume were determined by the BJH method.

Methyleneblue adsorption

The pollutant uptaking capacities of the different systems were studied by mixing with dye in a glass conical flask where the contents were uniformly stirred. 50 mL of MB was placed in the glass flask, containing a definite amount of the adsorbent and is continuously stirred at room temperature. The MB concentration of the solution was analyzed using a colorimeter (ESICO Microprocessor photo colorimeter model 1312) at a wavelength of 665 nm. The influence of reaction variables such as, the adsorbent weight, dye concentration, CoSBA weight ratio, etc., were investigated for better results. The adsorption studies were also conducted over the physical blend of Co and SBA 15. The reusability of 10 wt% Co-doped systems is done by removing the dye after adsorption by treating at 500 °C for 1 h.

Results and discussion

Material characterization

The nature of cobalt over the support is studied using different characterization techniques. X-ray diffraction patterns of the present systems (Fig. 1) showed amorphous silica and crystalline spinel cobalt oxide, Co_3O_4 (Thackeray et al. 1982). Ma et al. (2007) had reported preparation and catalytic activity of Co/SBA where ethanolic solution of $Co(OAc)_2$ is impregnated over SBA 15. They suggested the formation of amorphous CoO as the cobalt phase.

In the case of our samples, the peaks are found to be weak at low concentrations of metal and cobalt exists only in its spinel structure. The spinel type cubic structure of Co_3O_4 is verified by the observation of the well defined diffraction peaks at $2\theta = 19.0°$, 31.3°, 36.8°, 44.8°, 59.2°, and 65.1°. With increase in the metal percentage, the peaks become narrow and intense. The color of the samples is found to be black, supporting the presence of cobalt in its spinel form (Szegedi et al. 2009). The crystallite size of the Co_3O_4 spinel is calculated using the peak around 2θ value of 36.8° by Scherrer equation. It is found that there is a regular trend of increasing crystallite size with increase in metal loading. Among the different systems, 5 % cobalt-loaded system show least crystallite size (Table 1).

FTIR spectra of samples (Fig. 2) show the absorption bands at around 660 and 555 cm^{-1} which are due to the fingerprint IR absorptions of Co_3O_4 (Nkeng et al. 1996). The intensity of these two peaks increases with cobalt content. The peaks of SBA 15 at around 470, 799, and 1,090 cm^{-1} corresponded to rocking, bending, and asymmetric stretching of the inter-tetrahedral oxygen atoms in the SiO_2 structure, respectively, are found to be retained (Xia et al. 2008), showing the retention of the mesoporous structure even after a metal loading of 50 %. Thus, from XRD analysis and FTIR spectra, it is confirmed that the loaded cobalt metal exists exclusively in its spinel structure, Co_3O_4.

UV–Vis DRS studies were done to know the absorbance nature of the systems. The SBA 15 support, which is not showing any absorbance in the visible region, upon cobalt loading shows excellent visible light absorbance and is evident from the spectra shown in Fig. 3. CoSBA samples

Table 1 Crystallite size, % MB removal, and adsorption capacity under selected conditions for different systems

Adsorbent	% MB removal	Adsorption capacity (mg/g)	Crystallite size (nm)
SBA 15	62.66	10.4433	–
5CoSBA	96.97	16.1616	8.56
10CoSBA	100.00	16.6666	10.46
20CoSBA	95.45	15.9083	11.77
30CoSBA	62.12	10.3533	13.14
40CoSBA	15.15	2.5250	18.24
50CoSBA	83.33	13.8883	22.61
10CoSBA blend	86.36	14.9333	–

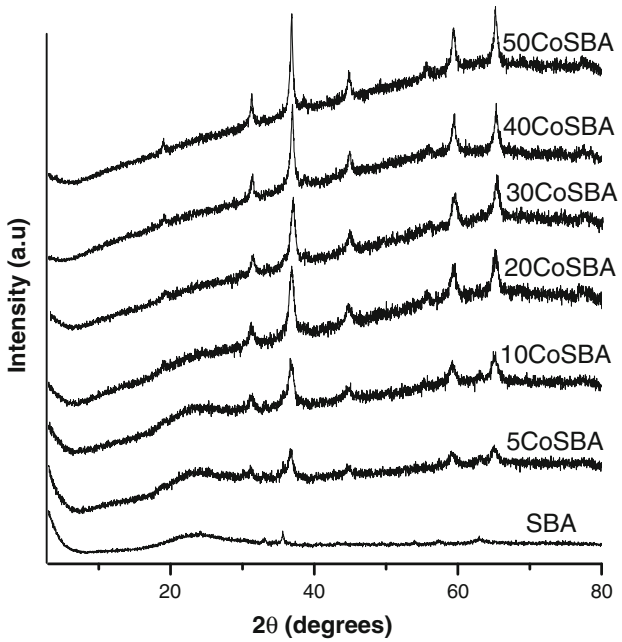

Fig. 1 XRD patterns of different systems

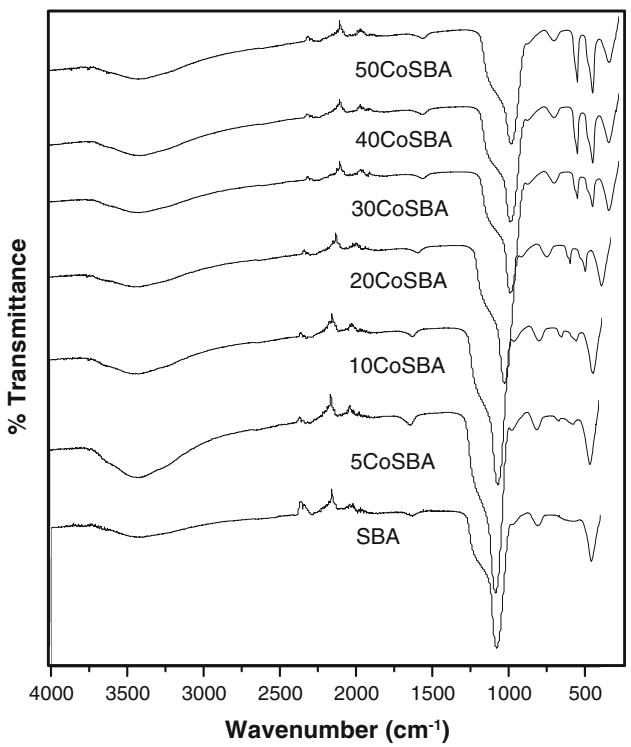

Fig. 2 FTIR spectra of cobalt loaded SBA 15 materials

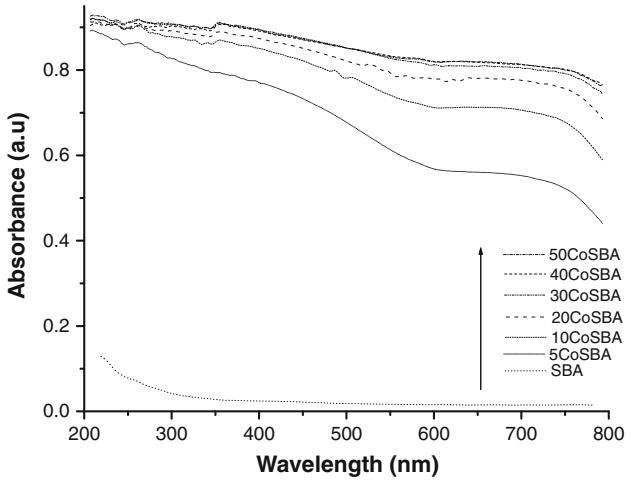

Fig. 3 UV–Vis DRS spectra of different adsorbents

showed increased absorption over a broad range of 400–700 nm compared with undoped SBA-15. The absorbance increases with loading and the spectra of 50CoSBA lies in the top among the spectra.

Representative TEM images obtained on Co-loaded adsorbents are shown in Fig. 4. Images show the highly ordered hexagonal arrangement of the channels along two directions, parallel, and perpendicular (not shown) to the *c* axis. The SBA-15-type structure was clearly maintained after cobalt impregnation and calcination. Owing to the electronic density contrasts, Co_3O_4 nanoparticles appear in black and silica walls in gray (Hassan et al. 2008). From the photographs, it can be seen that these oxide nanoparticles in the 10CoSBA samples are mainly trapped within the mesopores. There is a uniform distribution of nanoparticles. But, for the samples with low metal loading of 5 % as well as high loading than 10 % shows that cobalt was also distributed on the exterior surface of the support and the particle size distribution is wide. For a high cobalt loading of 40 (not shown) and 50 %, cobalt oxide species are agglomerated to form hexagonal structure on the surface of the support which consists of many small particles. In the case of 50 % loading, smaller particles are found to be absent. However, it is obvious that not all the channels in this sample are filled by cobalt oxide.

Fiber-like morphology of calcined SBA 15 materials is shown in SEM images (Fig. 5). The particles of the prepared SBA 15 were joined to form long fibrous macrostructures with a relative particle size of several micrometers (Zhao et al. 1998). Many rod-like subparticles with relatively uniform sizes aggregated into wheat-like macrostructures (Katiyar et al. 2006; Chao et al. 2002). All the cobalt-loaded systems retained this morphology and it

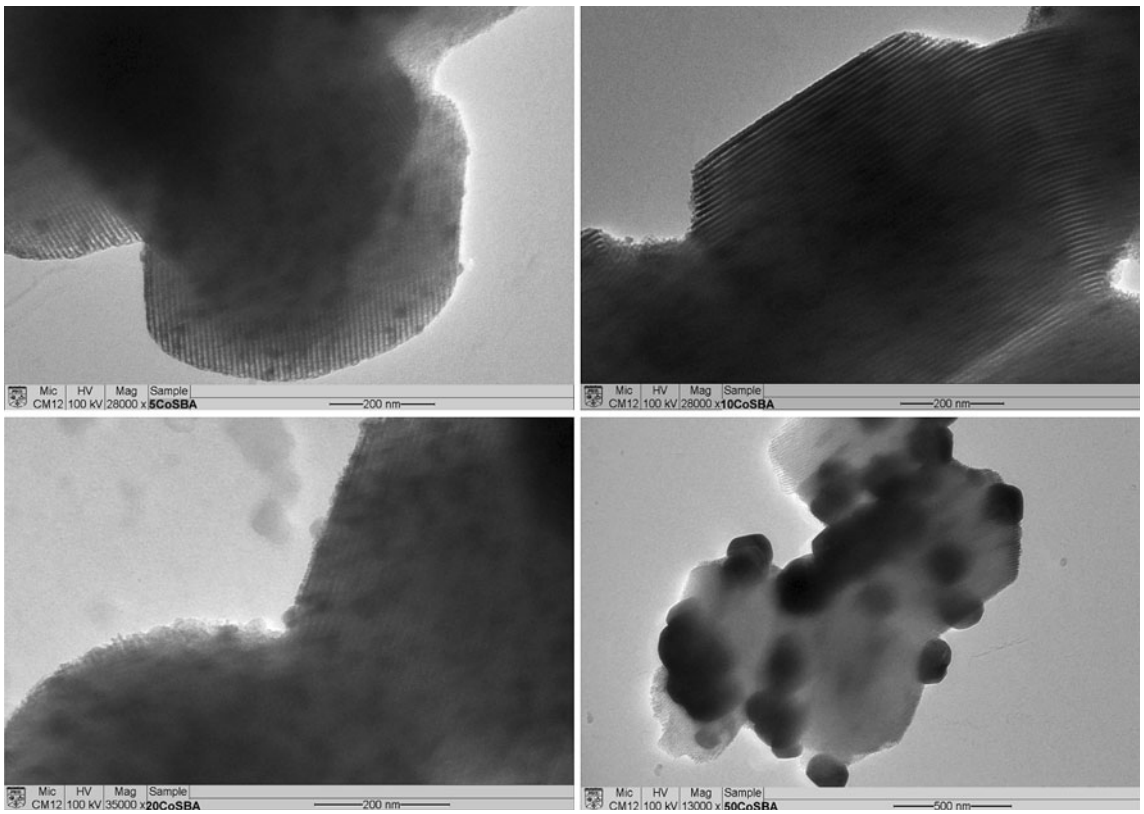

Fig. 4 TEM images of the prepared systems

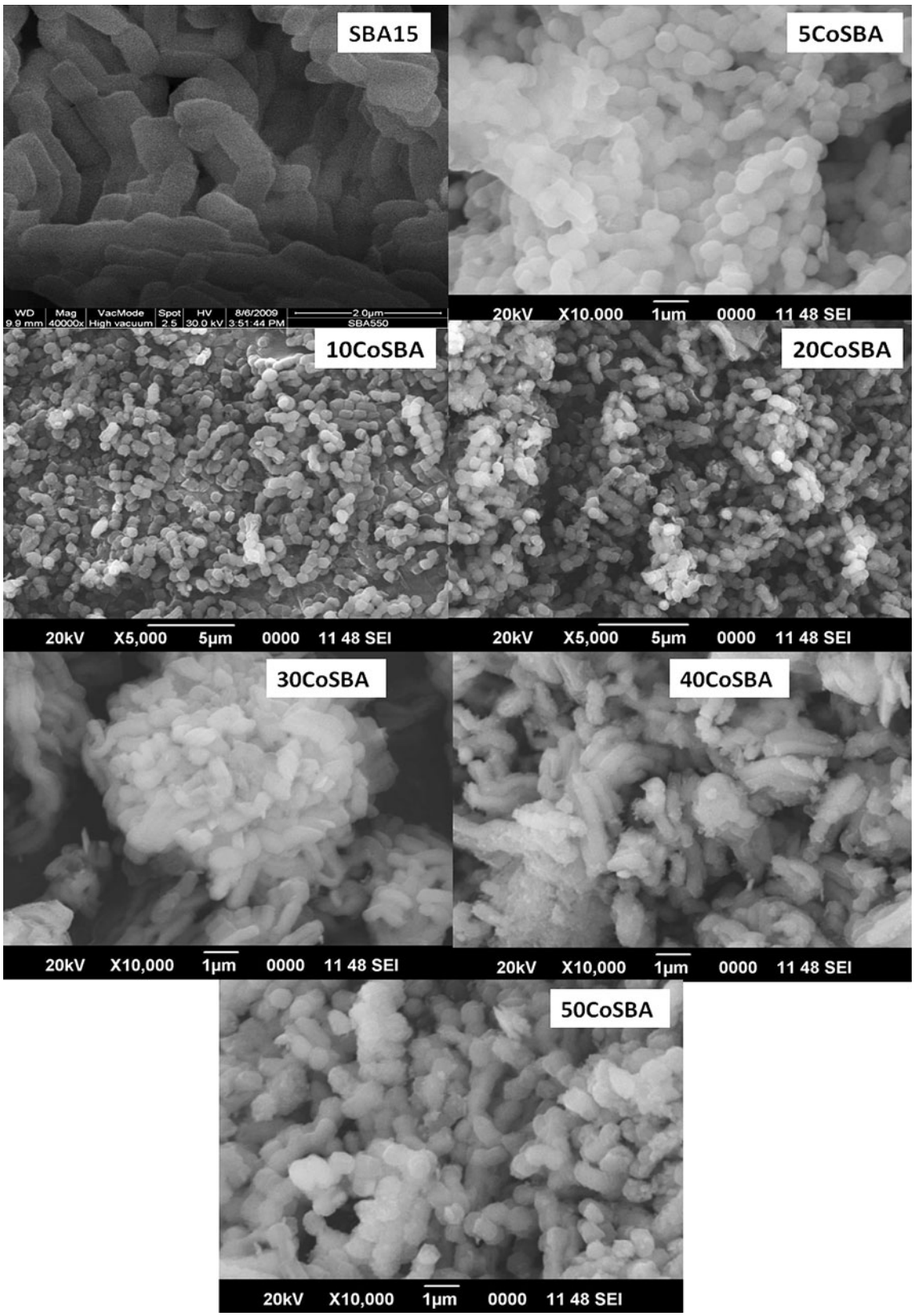

Fig. 5 SEM images of adsorbents

can be seen that there is no surface agglomeration of cobalt oxide particles.

Surface area and porosity data measurements of some representative samples were done by BET BJH method. The samples showed typical mesoporous structures which exhibit pronounced hysteresis loops similar to those commonly observed for conventional mesoporous silicas and are featured by the type IV isotherms. The prepared SBA 15 and Co-doped SBA systems exhibit H1 hysteresis loops, which indicate the presence of open-ended cylindrical pores lying in narrow range of radius (Fig. 6). Table 2 shows the BET surface area, pore volume, and average pore diameter of representative systems. Metal loading decreases the BET surface area and pore volume which may be due to plugging of the support pores by cobalt oxide. The plugging makes the pores inaccessible for nitrogen adsorption. This is consistent with the loss of specific surface area after metal loading due to the blocking of pore's entrance by the clusters of metal oxides. The pore volume reduction increases with metal loading even though surface area is not showing a decreasing trend with increase in the metal loading. The increase in the average pore diameter may be due to leaching out of some Si from the matrix (Tsoncheva et al. 2009).

Adsorption studies

All MB adsorption experiments were carried out under constant stirring using a magnetic stirrer. The use of SBA 15 as a support for Co_3O_4 insures efficient separation of the nanoparticles from the aqueous solution after adsorption. Since the systems show good visible light absorbance as seen from the UV DRS spectra, we also investigated the possibility of photodegradation of the dyes over the adsorbents by conducting the experiments in dark where the percentage dye removal remained same. To evaluate the comparative adsorptivity of our samples and to find out the best conditions, the system selected is 10CoSBA.

Effect of initial MB concentration

The dye in the effluent of different sources may have different concentrations and thus we studied the effect of initial MB concentration on the dye removal capacity of the Co/SBA adsorbents. The results shown in Fig. 7a show that the increment of initial dye concentration from 10 to 75 mg/L lead to a decrease in the adsorption of MB from 100 to 52.7 %. Up to 30 mg/L, it shows 100 % adsorption. Even for 50 mg/L, the system shows outstanding adsorptivity within 15 min. So, we selected the MB concentration of 50 mg/L for comparison of the adsorptivity of different systems. For studies on the change in dye concentration, the other parameters were kept constant, i.e., Co loading, time, and adsorbent weight. In that condition, the number of active sites available for adsorption remains constant. Therefore, with the increase in MB molecules for the same number of active sites, there is a decrease in percentage dye removal. But, up to a concentration of 30 mg/L, the active sites are sufficient for complete adsorption of MB within a small duration of 15 min time.

Effect of adsorbent dose on MB removal

Figure 7b shows the variety of dye removal rates of MB (50 mg/L) for a short interval of 15 min, as a function of

Table 2 Textural properties of supports and selected adsorbents

Adsorbent	BET surface area (m^2/g)	Pore volume (cm^3/g)	Pore diameter (nm)
SBA 15	527.2544	0.895074	5.9376
10CoSBA	315.5639	0.678986	6.8993
20CoSBA	320.0652	0.588541	6.1180

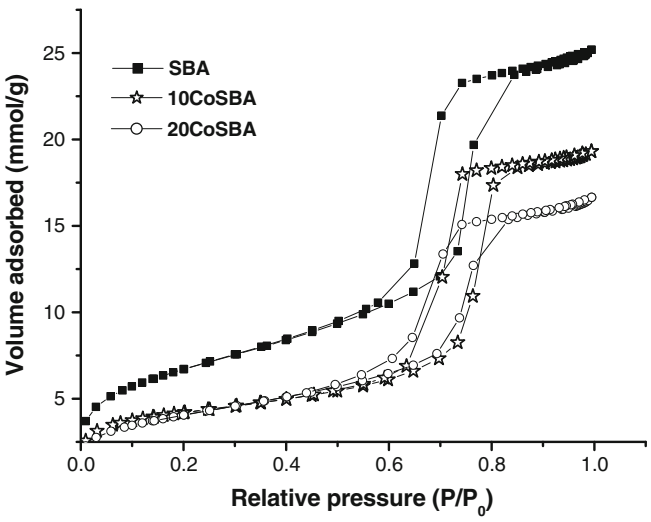

Fig. 6 Nitrogen adsorption desorption isotherms for the prepared systems

the adsorbent amount. It is apparent from the figure that with increase in the adsorbent dose of 10CoSBA, the uptake of MB increases up to an adsorbent dose of 3 g/L and reaches 100 %. Further increase in the dose does not affect MB adsorption. The initial marginal increase in the efficiency with adsorbent amount is because, initial concentration of MB solution is constant throughout the dose study. With increasing amount of adsorbent, the number of active sites of adsorption increases which in turn increases MB uptake. Then, the finest adsorbent loading is 3 g/L.

Effect of time

Figure 7c shows effect of time on percentage MB removal. The adsorption is done using 50 mg/L MB with 3 g/L 10CoSBA. It is observed that with the increase in time from 5 min to 10 min, the concentration of MB in the solution decreased to zero. Complete adsorption of MB occurs within a short duration of 10 min. Over the present system, a short duration of adsorption time of 10 min is found to be sufficient for the complete removal of aquatic pollutant, MB.

Effect of Co loading

Adsorbent systems with different Co loading were synthesized by changing the weight ratio of Cobalt with SBA. All these adsorbents were evaluated for MB adsorption under selected conditions. The decrease in MB concentration is observed to be 62.66 % for undoped SBA 15. The result of percentage MB removal over different systems with increasing Co loading under selected conditions and adsorption capacities of each systems are given in Table 1. 10CoSBA shows complete MB adsorption which decreases

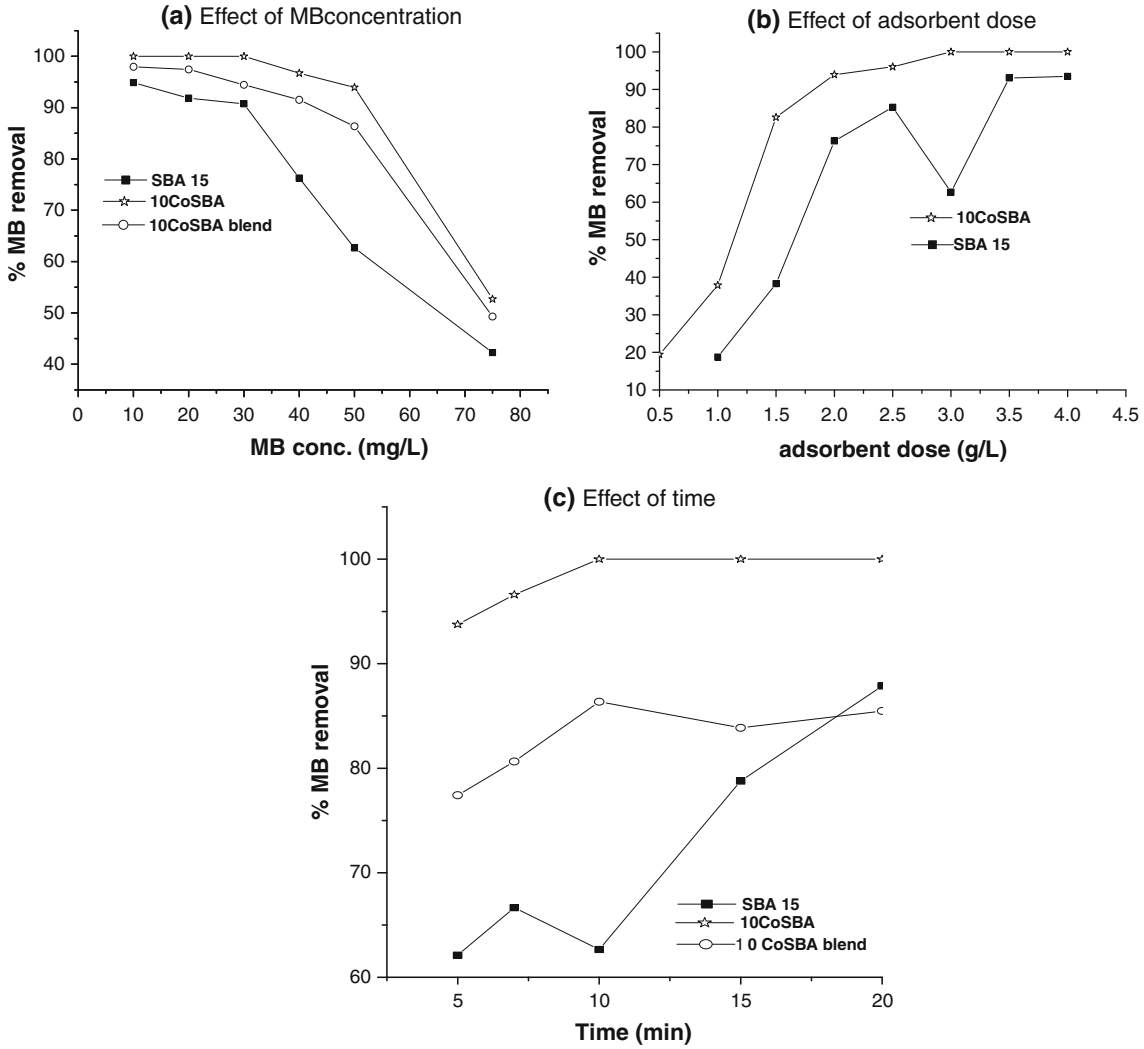

Fig. 7 Influence of reaction variables, **a** adsorbent dose = 3 g/L; time = 10 min; MB conc. = 50 mg/L; for 10CoSBA adsorbent dose = 2 g/L; time = 15 min; MB conc. = 50 mg/L; **b** time = 10 min; MB conc. = 50 mg/L; **c** adsorbent dose = 3 g/L; MB conc. = 50 mg/L

with further increase in Co loading and reaches minimum at an adsorbent loading of 40 %, but show drastic increase at 50 %. We tried to correlate the adsorptivity with the morphology of different systems because all systems are found to show the existence of Co in the form of Co_3O_4 spinel structure as evident from XRD and FTIR studies. As already discussed, representative TEM pictures show the exclusive existence of Co inside the pores of SBA 15 in 10CoSBA, whereas both internal as well as external surface-adhered cobalt oxide species are present on other systems. Thus, among the different systems, Co_3O_4 spinel that exists mainly in the mesopores of SBA 15 shows excellent response to MB when compared to that on the external surface. But, the anomalous trend in the adsorptivity shown by 50CoSBA may be due to the existence of well-dispersed hexagonal aggregates of the spinel. There are no smaller particles of Co_3O_4 present and only the big hexagonal clusters of Co_3O_4 are found over the system with 50 % Co loading.

The results reveal the relatively high dye removal capacity of the prepared adsorbents which enables the complete adsorption of the pollutant in such a short period of time.

In order to confirm the efficiency of the present adsorbent, the activity studies under different conditions are also done over SBA 15 and the physical blend of 10 wt% Co over SBA 15. The results are shown in Fig. 7. It can be seen that, SBA 15 is the weakest adsorbent and the blend is also showing lower performance than that of 10CoSBA, the best adsorbent of the present study. From the plot of influence of time, it can be assumed that the blend and SBA 15 shows a reversible nature on adsorption of dye, and thus there is a zig zag trend in the adsorption versus time. But, 10CoSBA did not show any reversible nature even after complete adsorption of dye from the solution. The results of reusability studies of 10 wt% Co incorporated systems are presented in Fig. 8. It can be seen that 10CoSBA shows promising performance of around 95 % adsorption even after four runs where there is a slight decrease in the adsorbing ability in continuous use. But, in the case of blend, from second cycle onwards the adsorbing power increases with increase in cycles. This may be due to the heat treatment obtained during regeneration of adsorbent sites, which may additionally homogenize the cobalt oxide over the SBA 15 support during this physical treatment. Still the activity is less than 10CoSBA.

The adsorptions of other dyes are also investigated over the best adsorbent 10CoSBA, the blend and SBA 15. Both blend and SBA 15 showed slightly lower adsorption capacity when compared to 10CoSBA. The adsorption of cationic dyes such as methylene blue, malachite green, and crystal violet are excellent whereas the present adsorbents failed to adsorb anionic or neutral dyes (Table 3). There

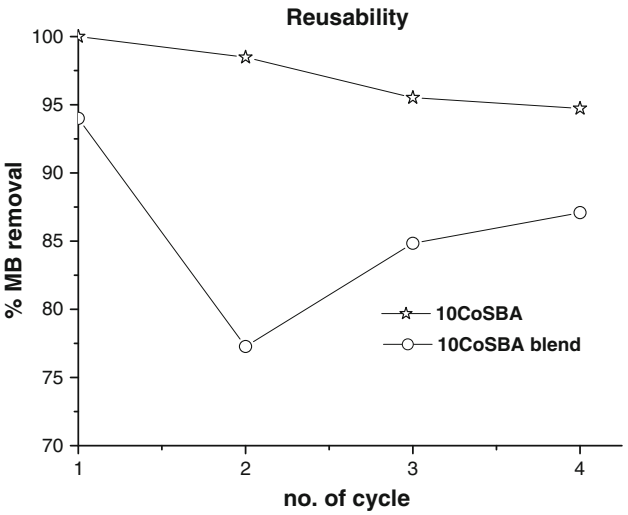

Fig. 8 Reusability studies of 10CoSBA and blend in the adsorption of 50 mL of 50 mg/L MB solution at an adsorbent dose of 3 g/L for 10 min mixing time

Table 3 Adsorption of different dyes under selected conditions of 50 mL of 50 mg/L dye solution at an adsorbent dosage of 3 g/L for 10 min mixing time

Dye	% adsorption		
	10CoSBA	10CoSBA blend	SBA 15
Malachite green	99.29	94.11	88.23
Crystal violet	99.08	97.91	98.95
Acid blue	17	–	–
Methylene blue	100	86.36	62.66

was no adsorption when the dyes were methyl orange and orange II, whereas very low amount of acid blue is adsorbed over 10CoSBA, but the blend and SBA could not adsorb any anionic or neutral dyes.

Conclusions

Effect of Cobalt loading on SBA 15 is characterized and its efficiency for the removal of methyleneblue dye via adsorption is investigated. Systems possess cobalt having spinel structure and are found to be better alternative adsorbents. Efficient dispersion of cobalt nanoparticles are seen from TEM pictures when the metal loading is low. Higher loading results in the agglomeration of Co_3O_4 nanoparticles to form hexagonal structure. Among the different systems, 10 wt% Co loading results in complete adsorption of dye pollutant within 10-min mixing time. Further studies on the kinetics of adsorption and its large scale applications are going on.

Acknowledgments The authors acknowledge the UKM, the grant number UKM-OUP-NBT-27-118/2009 for the financial support. STIC, CUSAT, Kochi, India, is acknowledged for XRD, FTIR, and UV–Vis DRS analysis.

References

Anbia M, Hariri SA (2010) Removal of methylene blue from aqueous solution using nanoporous SBA-3. Desalination 261:61–66. doi:10.1016/j.desal.2010.05.030

Apetrei R, Catrinescu C, Mardare D, Teodorescu CM, Luca D (2009) Photo-degradation activity of sputter-deposited nitrogen-doped Titania thin films. Thin Solid Films 518:1040–1043. doi:10.1016/j.tsf.2009.05.068

Asahi R, Morikawa T, Ohwaki T, Aoki K, Taga Y (2001) Visible-light photocatalysis in nitrogen-doped titanium oxides. Science 293:269–271. doi:10.1126/science.1061051

Chao MC, Lin HP, Sheu HS, Mou CY et al (2002) A study of morphology of mesoporous silica SBA-15. Stud Surf Sci Catal 141:387–394. doi:org/10.1016/S0167-2991(02)80566-3

Hassan NE, Davidson A, Costa PD, Mariadassou GD et al (2008) Methane activation by NO_2 on Co loaded SBA-15 catalysts: the effect of mesopores (length, diameter) on the catalytic activity. Catal Today 137:191–196. doi:10.1016/j.cattod.2008.01.020

He Z, Xie L, Song S, Wang C, Tu J, Hong F, Liu Q, Chen J, Xu X (2010) The impact of silver modification on the catalytic activity of iodine-doped titania for *p*-chlorophenol degradation under visible-light irradiation. J Mol Catal A 319:78–84. doi:10.1016/j.molcata.2009.12.003

Huang CH, Chang KP, Ou HD, Chiang YC, Wanga CF (2011) Adsorption of cationic dyes onto mesoporous silica. Microporous Mesoporous Mater 141:102–109. doi:10.1016/j.micromeso.2010.11.002

Joo JB, Park J, Yi J (2009) Preparation of polyelectrolyte-functionalized mesoporous silicas for the selective adsorption of anionic dye in an aqueous solution. J Hazard Mater 168:102–107. doi:10.1016/j.jhazmat.2009.02.015

Katiyar A, Yadav S, Smirniotis PG, Pinto NG et al (2006) Synthesis of ordered large pore SBA-15 spherical particles for adsorption of biomolecules. J Chromatogr A 1122:13–20. doi:10.1016/j.chroma.2006.04.055

Lee B, Ma Z, Zhang Z, Park C, Dai S et al (2009) Influences of synthesis conditions and mesoporous structures on the gold nanoparticles supported on mesoporous silica hosts. Microporous Mesoporous Mater 122:160–167. doi:10.1016/j.micromeso.2009.02.029

Ma H, Xu J, Chen C, Zhang Q, Ning J, Miao H, Zhou L, Li X (2007) Catalytic aerobic oxidation of ethylbenzene over Co/SBA-15. Catal Lett 113:104–108. doi:10.1007/s10562-007-9019-7

Moriguchi I, Honda M, Ohkubo T, Mawatari Y, Teraoka Y (2004) Adsorption and photocatalytic decomposition of methylene blue on mesoporous metallosilicates. Catal Today 90:297–303. doi:10.1016/j.cattod.2004.04.034

Nkeng P, Koening F, Gautier L, Chartier P, Poillerat G (1996) Enhancement of surface areas of Co_3O_4 and $NiCo_2O_4$ electrocatalysts prepared by spray pyrolysis. J ElectroanalChem 402:81-89. SSDI 0022-0728(95)04254-7

Peng F, Cai L, Yu H, Wang H, Yang J (2008) Synthesis and characterization of substitutional and interstitial nitrogen-doped titanium dioxides with visible light photocatalytic activity. J Solid State Chem 181:130–136. doi:10.1016/j.jssc.2007.11.012

Popa M, Macovei D, Indrea E, Mercioniu I, Popescu IC, Danciu V (2010) Synthesis and structural characteristics of nitrogen doped TiO_2 aerogels. Microporous Mesoporous Mater 132:80–86. doi:10.1016/j.micromeso.2009.12.024

Ren TZ, Yuan ZY, Su BL (2007) Encapsulation of direct blue dye into mesoporous silica-based materials. Colloid Surf A 300:79–87. doi:10.1016/j.colsurfa.2006.12.054

Szegedi A, Popova M, Minchev C (2009) Catalytic activity of Co/MCM-41 and Co/SBA-15 materials in toluene oxidation. J Mater Sci 44:6710–6716. doi:10.1007/s10853-009-3600-y

Thackeray MM, David WIF, Goodenough JB (1982) Structural characterization of the lithiated iron oxides $Li_xFe_3O_4$ and $Li_xFe_2O_3$ ($0 < x < 2$). Mater Res Bull 17:785–793. doi:10.1016/0025-5408(82)90029-0

Tsoncheva T, Ivanova L, Rosenholm J, Linden M et al (2009) Cobalt oxide species supported on SBA-15, KIT-5 and KIT-6 mesoporous silicas for ethyl acetate total oxidation. Appl Catal B 89:365–374. doi:org/10.1016/j.apcatb.2008.12.015

Wang S, Li H (2006) Structure directed reversible adsorption of organic dye on mesoporous silica in aqueous solution. Microporous Mesoporous Mater 97:21–26. doi:10.1016/j.micromeso.2006.08.005

Wang J, Wang Z, Li H, Cui Y, Du Y (2010) Visible light-driven nitrogen doped TiO_2nanoarray films: Preparation and photocatalytic activity. J Alloys Compd 494:372–377. doi:10.1016/j.jallcom.2010.01.049

Xia F, Ou E, Wang L, Wang J (2008) Photocatalytic degradation of dyes over cobalt doped mesoporous SBA-15 under sunlight. Dyes Pigments 76:76–81. doi:10.1016/j.dyepig.2006.08.008

Zhao DY, Feng JL, Huo QS, Melosh N, Fredrickson GH, Chmelka BF, Stucky GD (1998) Triblock copolymer syntheses of mesoporous silica with periodic 50 to 300 angstrom pores. Science 279:548–552. doi:10.1126/science.279.5350.548